

Internal quantum efficiency and nonradiative recombination coefficient of GaInN/GaN multiple quantum wells with different dislocation densities

Q. Dai,¹ M. F. Schubert,¹ M. H. Kim,¹ J. K. Kim,¹ E. F. Schubert,^{1,a)} D. D. Koleske,² M. H. Crawford,² S. R. Lee,² A. J. Fischer,² G. Thaler,² and M. A. Banas²

¹Department of Physics, Applied Physics, and Astronomy and Department of Electrical, Computer, and Systems Engineering, Future Chips Constellation, Rensselaer Polytechnic Institute, Troy, New York 12180, USA

²Sandia National Laboratories, Albuquerque, New Mexico 87185, USA

(Received 20 November 2008; accepted 27 February 2009; published online 17 March 2009)

Room-temperature photoluminescence (PL) measurements are performed on GaInN/GaN multiple-quantum-well heterostructures grown on GaN-on-sapphire templates with different threading-dislocation densities. The selective optical excitation of quantum wells and the dependence of integrated PL intensity on excitation power allow us to determine the internal quantum efficiency (IQE) as a function of carrier concentration. The measured IQE of the sample with the lowest dislocation density ($5.3 \times 10^8 \text{ cm}^{-2}$) is as high as 64%. The measured nonradiative coefficient A varies from 6×10^7 to $2 \times 10^8 \text{ s}^{-1}$ as the dislocation density increases from 5.3×10^8 to $5.7 \times 10^9 \text{ cm}^{-2}$, respectively. © 2009 American Institute of Physics.

[DOI: [10.1063/1.3100773](https://doi.org/10.1063/1.3100773)]

GaN/GaN multiple-quantum-well (MQW) light-emitting diodes (LEDs) are highly efficient semiconductor sources of short-wavelength visible light. However, the direct and accurate measurement of the MQW internal quantum efficiency (IQE) as a function of carrier concentration remains to be a continuing challenge. Previously, the IQE of III-V semiconductor QWs has been determined by absolute intensity measurements using an integrating sphere,¹ a steady-state thermal study,² time-resolved photoluminescence (PL),³ temperature-dependent relative IQE measurements,^{4,5} and methods based on a semiconductor rate equation analysis.^{6–8} In the present work, we determine the IQE of GaInN/GaN MQWs from the dependence of integrated PL intensity on excitation power.⁶ We apply this technique to a series of MQW samples with different threading-dislocation densities and establish both the IQE versus carrier concentration and the nonradiative coefficient A . Our PL measurements employ selective optical pumping of the GaInN QW layers to avoid carrier generation in the barrier layers and reduce carrier transport effects. This delineation is of interest to more clearly isolate recombination processes in GaInN MQWs, given the potential for carrier injection and carrier leakage to contribute to the “efficiency droop” in electroluminescence (EL)-based measurements of GaInN-based LEDs at high carrier densities.^{9–11}

The GaInN/GaN MQW LED heterostructures are grown on GaN-on-sapphire templates by metal-organic vapor-phase epitaxy. The threading-dislocation densities of the templates are controlled by varying nucleation-layer-growth and film-coalescence parameters.^{10,12,13} Threading-dislocation densities are evaluated using x-ray diffraction (XRD) rocking-curve measurements of the Bragg peak widths of the (0004) and (10 $\bar{1}$ 1) reflections of GaN. Threading-dislocation densities are extracted from the measured peak widths using equations described in Ref. 14. For the edge-type threading dislocations predominating in typical GaN-on-sapphire tem-

plates, previous work finds that these XRD measurements of threading-dislocation density agree with transmission electron microscopy to within a standard error of $\sim 33\%$.¹⁴ To avoid extrinsic sources of IQE variation, the LED epistructures are grown in the same growth run on three different templates. The MQW structure has five 2.4-nm-thick Ga_{0.87}In_{0.13}N QWs sandwiched between 7.5-nm-thick Si-doped GaN quantum barriers, followed by a 30-nm-thick p -type Al_{0.15}Ga_{0.85}N electron-block layer and a 400-nm-thick p -type GaN contact layer.¹⁰ For the three resulting LED wafers in this study, named A, B, and C, we have measured total threading-dislocation densities of 5.7×10^9 , 1.2×10^9 , and $5.3 \times 10^8 \text{ cm}^{-2}$, respectively.

Our PL studies employ a 405 nm laser diode as an excitation source to enable photoexcited carrier generation only in the GaInN QWs. By applying this exclusive QW excitation, we avoid optical carrier generation in the barrier layers and reduce carrier transport effects occurring in EL measurements. The laser diode is operated in a pulsed mode, with a 100 μs period and 1% duty cycle. To vary the carrier concentration, the laser diode injection current is increased from 50 to 180 mA, with a 10 mA interval, producing incident peak power densities ranging from 0.21 to 1.88 kW/cm².

The resulting MQW emission spectra are modulated by a periodic interference term, as shown by three representative spectra that result from each of our three samples in Fig. 1(a). The interference is caused by the formation of an optical resonator formed by the GaN/sapphire and GaN/air interfaces. Our measurements show that the spectra of GaInN/GaN MQWs grown on GaN substrates⁹ have no such interference and can be fitted very well by a Lorentzian distribution, as shown by Fig. 1(b). Given this clear underlying dependence, we obtain integrated PL intensities by fitting our modulated spectra to a Lorentzian distribution. Figure 1(a) also shows the corresponding Lorentzian fits for the three spectra. To avoid the laser-emission tail during spectral fitting and integration, a limited PL-wavelength range from 425 to 500 nm is used.

^{a)}Electronic mail: efschubert@rpi.edu.

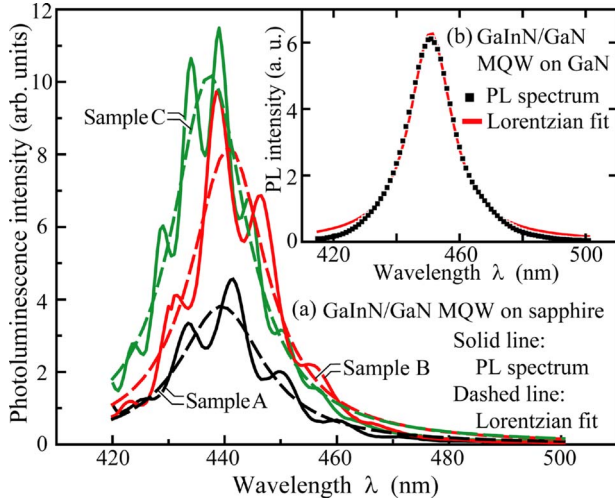


FIG. 1. (Color online) (a) Representative spectra and the corresponding Lorentzian fits for three samples with varying dislocation densities and (b) (insert) a representative spectrum and a Lorentzian fit for a GaInN/GaN MQW LED heterostructure grown on a bulk-GaN substrate.

Next, we present a theoretical model. The three main carrier-recombination mechanisms in a bulk semiconductor are Shockley–Read–Hall nonradiative recombination, expressed as An , bimolecular radiative recombination Bn^2 , and Auger nonradiative recombination Cn^3 , where A , B , and C are the respective recombination coefficients and n is the carrier concentration. Auger recombination affects LED efficiency only at very high excitation; thus, in our experiments, the generation rate and the IQE at steady state can be expressed as

$$G = R_{\text{total}} = An + Bn^2, \quad (1)$$

$$\text{IQE} = Bn^2 / (An + Bn^2) = Bn^2 / G, \quad (2)$$

and the integrated PL intensity can be expressed as

$$I_{\text{PL}} = \eta Bn^2, \quad (3)$$

where η is a constant determined by the volume of the excited active region and the total collection efficiency of luminescence. By eliminating n in Eqs. (1) and (3), we can express the generation rate in terms of integrated PL intensity

$$G = \frac{A}{\sqrt{B\eta}} \sqrt{I_{\text{PL}}} + \frac{1}{\eta} I_{\text{PL}}. \quad (4)$$

The connection between theory and experiment is completed by noting that the generation rate can be separately calculated from experimental parameters using

$$G = P_{\text{laser}}(1 - R)\alpha l / (A_{\text{spot}} h\nu) = P_{\text{laser}}(1 - R)\alpha / (A_{\text{spot}} h\nu), \quad (5)$$

where P_{laser} is the peak optical power incident on the sample, R (18%) is the Fresnel reflection at the sample surface, l (12 nm) is the total thickness of the GaInN QWs, A_{spot} ($3.5 \times 10^3 \mu\text{m}^2$) is the area of the laser spot on the sample surface, $h\nu$ (3.07 eV) is the energy of a 405 nm photon, and α ($5.4 \mu\text{m}^{-1}$) is the absorption coefficient of the $\text{Ga}_{0.87}\text{In}_{0.13}\text{N}$ well at 405 nm. The absorption coefficient is calculated from its square-root dependence on energy¹⁵

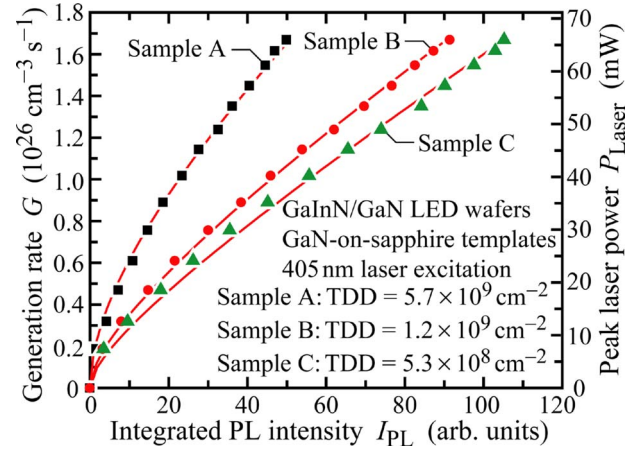


FIG. 2. (Color online) Generation rate G as a function of integrated PL intensity I_{PL} and fitted curves obtained using Eq. (4).

$$\alpha = \alpha_0 \sqrt{(E - E_g) / E_g}, \quad (6)$$

where α_0 is the absorption coefficient at $h\nu = 2E_g$, is obtained by linear interpolation between GaN and InN [we use $\alpha_0 = 2.0 \times 10^5 \text{ cm}^{-1}$ for GaN and $\alpha_0 = 1.2 \times 10^5 \text{ cm}^{-1}$ for InN (Ref. 15)]. Figure 2 shows the experimental results for G as a function of I_{PL} obtained using Eq. (5) and our previous fits of the spectral data. Using Eq. (4) to fit the experimental data in Fig. 2, we then obtain the coefficients $P_1 = A(B\eta)^{-1/2}$ and $P_2 = 1/\eta$. Because the samples have the same layer structure and are measured under the same conditions, the values of P_2 (or η) for the three samples should be the same or similar. Therefore we keep the values of P_2 fixed for the three samples while fitting the data. The fitted results, also shown in Fig. 2, are excellent; thus Eq. (4) appears to accurately model our experiments.

We are now positioned to extract IQEs, carrier concentrations, and the nonradiative recombination coefficients from the fitted data. Eliminating A from $P_1 = A(B\eta)^{-1/2}$ and Eq. (1) yields

$$G = P_1 \sqrt{\eta} \sqrt{Bn} + (\sqrt{Bn})^2. \quad (7)$$

By solving Eq. (7) for $B^{1/2}n$ and inserting into Eq. (2), the IQE is obtained. At the highest excitation, which has a generation rate of $1.7 \times 10^{26} \text{ cm}^{-3} \text{ s}^{-1}$, the IQEs are 31%, 55%, and 64% for samples A, B, and C, respectively. If one assumes a value of B at room temperature of $1 \times 10^{-10} \text{ cm}^3/\text{s}$,^{7,15} the value of carrier concentration n can also be obtained. By eliminating η from the two coefficients P_1 and P_2 , one can obtain the value of $A(B)^{-1/2}$ and finally, the coefficient A . Considering the fact that B is known to only one significant figure, the accuracy of A and n are similarly limited. In Fig. 3(a), we present the measured IQE as a function of carrier concentration n for the three samples. Our results demonstrate higher radiative efficiencies at a given carrier concentration for the samples with lower dislocation density. Figure 3(b) shows the measured nonradiative coefficient A as a function of dislocation density, including values of 2×10^8 , 8×10^7 and $6 \times 10^7 \text{ s}^{-1}$ for samples A, B, and C, respectively. Both Figs. 3(a) and 3(b) indicate that the threading-dislocation density significantly affects the GaInN MQW efficiency, which supports the argument that threading dislocations behave as nonradiative recombination centers.¹⁶ On the other hand, the measured IQE is very high (up to

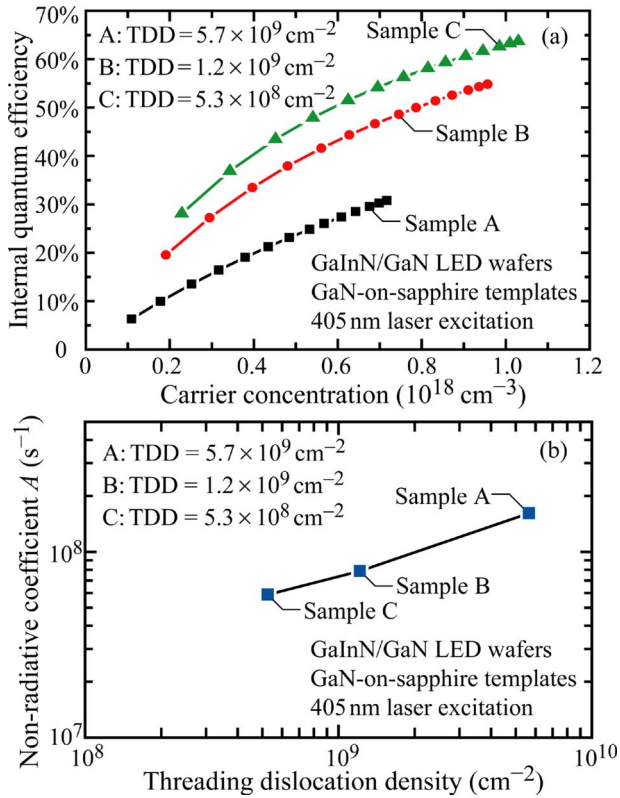


FIG. 3. (Color online) (a) Internal quantum efficiency as a function of carrier concentration and (b) nonradiative coefficient A as a function of threading-dislocation density.

64%). Chichibu *et al.*¹⁷ postulated that threading dislocations act as nonradiative channels, but strong spatial localization effectively suppresses the QW excitons from being trapped into threading dislocations, leading to highly efficient emissions from GaInN based devices. An upper limit for the Auger coefficient C is estimated to be about $2.7 \times 10^{-30} \text{ cm}^6 \text{ s}^{-1}$ for GaInN material and the actual value may be smaller.¹⁸ Therefore in our experiments, the Cn^3 term is much less than the Bn^2 term considering that the carrier concentration in our experiments is less than $1 \times 10^{18} \text{ cm}^{-3}$, in agreement with our assumption in Eq. (1).

Recently it was shown that leakage of carriers from GaInN QWs may occur even when the energy of optical excitation is much less than the bandgap energy of GaN quantum barrier.¹⁹ This leakage could affect the analysis presented here. We are further studying this effect to quantitatively assess the effect of carrier leakage on our results.

In conclusion, room-temperature power-dependent PL measurements are performed on GaInN/GaN MQW LED heterostructures grown on GaN-on-sapphire templates with different threading-dislocation densities. A 405 nm laser diode source is used for selective excitation of GaInN MQWs and determination of both the IQE as a function of carrier

concentration n and nonradiative coefficient A . Our studies establish a high IQE of 64% at a carrier concentration of $1 \times 10^{18} \text{ cm}^{-3}$ for the sample with the lowest dislocation density ($5.3 \times 10^8 \text{ cm}^{-2}$). The measured nonradiative recombination coefficient A varies from 6×10^7 to $2 \times 10^8 \text{ s}^{-1}$ as the dislocation density increases from 5.3×10^8 to $5.7 \times 10^9 \text{ cm}^{-2}$, respectively, confirming the nonradiative nature of these defects.

The RPI authors thank Sandia National Laboratories, the National Science Foundation, New York State, Samsung Electro-Mechanics Co., Crystal IS, and Troy Research Corporation. The Sandia authors acknowledge the DOE Office of Basic Energy Sciences and the Laboratory Directed Research and Development program for partial funding of this study. Sandia is a multiprogram laboratory operated by Sandia Corporation, a Lockheed Martin Co., for the United States Department of Energy's National Nuclear Security Administration under Contract No. DE-AC04-94AL85000.

- ¹T. Fleck, M. Schmidt, and C. Klingshirn, *Phys. Status Solidi A* **198**, 248 (2003).
- ²H. Gauck, T. H. Gfroerer, M. J. Renn, E. A. Cornell, and K. A. Bertness, *Appl. Phys. A: Mater. Sci. Process.* **64**, 143 (1997).
- ³R. K. Ahrenkiel, *Solid-State Electron.* **35**, 239 (1992).
- ⁴C. E. Martinez, N. M. Stanton, A. J. Kent, D. M. Graham, P. Dawson, M. J. Kappers, and C. J. Humphreys, *J. Appl. Phys.* **98**, 053509 (2005).
- ⁵S. Watanabe, N. Yamada, M. Nagashima, Y. Ueki, C. Sasaki, Y. Yamada, T. Taguchi, K. Tadatomo, H. Okagawa, and H. Kudo, *Appl. Phys. Lett.* **83**, 4906 (2003).
- ⁶D. Ding, S. R. Johnson, J. B. Wang, S. Q. Yu, and Y. H. Zhang, *Proc. SPIE* **6841**, 68410D (2007).
- ⁷H. Y. Ryu, K. H. Ha, J. H. Chae, K. S. Kim, J. K. Son, O. H. Nam, Y. J. Park, and J. I. Shim, *Appl. Phys. Lett.* **89**, 171106 (2006).
- ⁸G. B. Ren, H. Summers, P. Blood, R. Perks, and D. Bour, *Proc. SPIE* **4283**, 78 (2001).
- ⁹M. H. Kim, M. F. Schubert, Q. Dai, J. K. Kim, E. F. Schubert, J. Piprek, and Y. Park, *Appl. Phys. Lett.* **91**, 183507 (2007).
- ¹⁰M. F. Schubert, S. Chhajed, J. K. Kim, E. F. Schubert, D. D. Koleske, M. H. Crawford, S. R. Lee, A. J. Fischer, G. Thaler, and M. A. Banas, *Appl. Phys. Lett.* **91**, 231114 (2007).
- ¹¹X. Ni, Q. Fan, R. Shimada, U. Ozgur, and H. Morkoc, *Appl. Phys. Lett.* **93**, 171113 (2008).
- ¹²D. D. Koleske, A. J. Fischer, A. A. Allerman, C. C. Mitchell, K. C. Cross, S. R. Kurtz, J. J. Figiel, K. W. Fullmer, and W. G. Breiland, *Appl. Phys. Lett.* **81**, 1940 (2002).
- ¹³D. D. Koleske and S. R. Lee (unpublished).
- ¹⁴S. R. Lee, A. M. West, A. A. Allerman, K. E. Waldrip, D. M. Follstaedt, P. P. Provencio, D. D. Koleske, and C. R. Abernathy, *Appl. Phys. Lett.* **86**, 241904 (2005).
- ¹⁵E. F. Schubert, *Light-Emitting Diodes*, 2nd ed. (Cambridge University Press, Cambridge, 2006).
- ¹⁶J. S. Speck and S. J. Rosner, *Physica B* **273**, 24 (1999).
- ¹⁷S. F. Chichibu, H. Marchand, M. S. Minsky, S. Keller, P. T. Fini, J. P. Ibbetson, S. B. Fleischer, J. S. Speck, J. E. Bowers, E. Hu, U. K. Mishra, S. P. DenBaars, T. Deguchi, T. Sota, and S. Nakamura, *Appl. Phys. Lett.* **74**, 1460 (1999).
- ¹⁸P. G. Eliseev, M. Osin'ski, H. Li, and I. V. Akimova, *Appl. Phys. Lett.* **75**, 3838 (1999).
- ¹⁹M. F. Schubert, J. Xu, Q. Dai, F. W. Mont, J. K. Kim, and E. F. Schubert, *Appl. Phys. Lett.* **94**, 081114 (2009).